



0016-7037(95)00083-6

## Modeling the sulfur and oxygen isotopic composition of sulfates through a halite-potash sequence: Implications for the hydrological evolution of the Upper Eocene Southpyrenean Basin

CARLOS AYORA,<sup>1</sup> CONXITA TABERNER,<sup>1</sup> CATHERINE PIERRE,<sup>2</sup> and JUAN-JOSÉ PUEYO<sup>3</sup><sup>1</sup>Institut de Ciències de la Terra (J. Almera), CSIC, Barcelona, Spain<sup>2</sup>Laboratoire d'Océanographie Dynamique, Université Pierre et Marie Curie, Paris, France<sup>3</sup>Departament de Geoquímica, Universitat de Barcelona, Barcelona, Spain

(Received January 25, 1994; accepted in revised form January 18, 1995)

**Abstract**—The isotopic composition of sulfates sampled throughout a complete evaporite sequence has contributed to the understanding of the evolution of the Southpyrenean Upper Eocene basin. The  $\delta^{34}\text{S}$  and  $\delta^{18}\text{O}$  values appear to be constant in thick segments of the sequence. This pattern is clearly different from the continuous decrease in  $\delta$  values predicted by the evaporation processes in a closed system. The observed trend of the  $\delta^{34}\text{S}$  and  $\delta^{18}\text{O}$  values can be successfully modeled by an evaporation process in an open system, where steady state conditions are reached, separated by periods of significant changes in the hydrological regime of the basin. Moreover, in the segments of the sequence where they are constant, the  $\delta^{34}\text{S}$  and  $\delta^{18}\text{O}$  values help to constrain the hydrological parameters of the model.

A first marine stage of the evolution of the basin corresponds to the formation of the Basal Anhydrite and Lower Halite Units. The mineral sequence corresponds to evaporation in a basin with a progressive degree of restriction and evaporation compensated by equal inflow of major marine origin. The sharp decrease in the  $\delta^{34}\text{S}$  and particularly the  $\delta^{18}\text{O}$  values, recorded at the end of the Basal Anhydrite Unit, illustrates a limited reservoir effect produced by the increase of restriction leading to the halite precipitation. The modeling of the constant isotopic values through the Lower Halite Unit confirms the isotopic composition of Eocene marine dissolved sulfate ( $\delta^{34}\text{S} = +20.0\text{‰}$ ;  $\delta^{18}\text{O} = +8.7\text{‰}$ ) deduced from the average values of marginal gypsum.

The second continental stage of basin evolution corresponds to the formation of the Potash Unit and the Upper Halite Unit. The mineral sequence and lateral extension indicate that the basin evolved with a decreasing brine volume after disconnection from the sea. The dilution of the residual brine stopped the precipitation of camallite, and the basin then evolved as a perennial endorreic lake with continental recharge replacing evaporation. The sharp decrease in the  $\delta^{34}\text{S}$  and  $\delta^{18}\text{O}$  values in the sylvite member is consistent with the massive precipitation of sulfate occurring during the decrease in the volume of water. The  $\delta$  values of the sulfates intercalated in the camallite and the Upper Halite Unit indicate the influence of the recycling of both the already deposited Upper Eocene sulfates and the Upper Triassic sulfates carried by continental recharge. The constant  $\delta^{34}\text{S}$  and  $\delta^{18}\text{O}$  values from the uppermost half of the Upper Halite Unit is used to constrain the sulfate source as 80% recycled Upper Triassic and 20% recycled Eocene gypsum.

### INTRODUCTION

The isotopic composition of sulfates from marine evaporite series has been used to constrain the variation through time of  $\delta^{34}\text{S}$  and  $\delta^{18}\text{O}$  of sulfate dissolved in the oceans on a world-wide scale (Nielsen and Ricke, 1964; Thode and Monster, 1965; Holser and Kaplan, 1966; Claypool et al., 1980). The variation in  $\delta^{34}\text{S}$  of sulfates through time is a consequence of large scale transfer from different sulfur reservoirs and reflects the sulfur global cycle (Holser and Kaplan, 1966; Nielsen et al., 1991). Since the earliest extensive isotopic studies, two facts have arisen: (1) older evaporites can be dissolved and deposited into younger evaporite basins and (2) the isotopic composition of sulfates intercalated in evaporite series shows a trend to lighter  $\delta^{34}\text{S}$  values in highly evaporated facies. Some of the first studies concerning the effect of evaporite recycling are those from Nielsen (1972) that interpreted the  $\delta^{34}\text{S}$  of sulfates in the Rhine graben as the influence of older evaporites. Birnbaum and Coleman (1979) also used  $\delta^{34}\text{S}$  values to interpret the origin of Oligocene continental evaporites from the Ebro Basin as being recycled from Triassic evapo-

rites. More recently, Fontes et al. (1991) and Utrilla et al. (1992) have shown that coupling  $\delta^{34}\text{S}$  and  $\delta^{18}\text{O}$  is a useful tool in detecting the recycling of older evaporites.

Sulfates intercalated with highly evaporated facies have  $\delta^{34}\text{S}$  values lighter than evaporite facies that precipitated during initial evaporation stages. There is not an agreement regarding the cause for such a decrease in the isotopic composition in the previous literature. Nielsen and Ricke (1964) interpret it as a consequence of diffusion in a salinity-stratified basin, while Holser and Kaplan (1966), Nielsen (1972, 1978), and Claypool et al. (1980) propose the decrease to result from sulfur isotope fractionation during crystallization in a closed system that follows a Rayleigh-like process with a fractionation factor slightly higher than one ( $\alpha = 1.00165$ , calculated by Thode and Monster, 1965). Raab and Spiro (1991) suggested this explanation to be valid up to the end of the halite facies only, and proposed from experimental data an  $\alpha$  value slightly higher than 1 for the sulfur of anhydrites from the halite field. Moreover, the last authors suggested a fractionation factor lower than 1 for the sulfur of minerals precipitating in the highly evaporated facies.

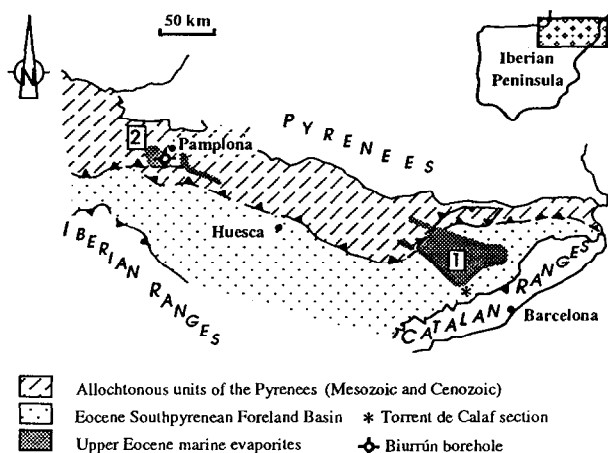


FIG. 1. Main areas with outcropping or mined evaporite deposits from the Upper Eocene basin of the Southpyrenean Foreland: (1) Catalonia depocenter and (2) Navarra depocenter. The map shows also the location of Biurrun borehole and the Torrent de Calaf section where the marginal evaporites have been sampled.

Within the same evaporite basin a variation in  $\delta^{34}\text{S}$  and  $\delta^{18}\text{O}$  values of sulfates is also expected as result of the recycling of older evaporites or from oxidized sulfides cropping out in the source area of the basin, together with the effect of fractionation during precipitation and the possible effect of a change in the fractionation factor at the onset of precipitation. The dispersion of the  $\delta^{18}\text{O}$  values of sulfate will be enhanced when redox processes occur in the evaporite basin itself (Pierre, 1985, 1989), as oxidation of sulfide depends both on the molar fraction and on the  $\delta^{18}\text{O}$  values of water and dissolved oxygen (Taylor et al., 1984; Van Everdingen and Krouse, 1985; Fritz et al., 1989). Therefore, the wide variation in isotopic data from a single evaporite basin may be a record of different physicochemical processes that makes difficult (1) the recognition of each one of these processes and (2) the adscription of an evaporite deposit to a certain age according to the accepted age curves of sulfur and oxygen from Holser and Kaplan (1966) and Claypool et al. (1980).

This paper presents the results of coupling a numerical model to the isotopic composition variation of sulfates intercalated in an evaporite sequence that includes highly evaporated facies. Unlike previous calculations of isotopic variations with evaporation progressing in a closed system, the model is based in a hydrologically open basin where evaporation and recharge from different sources take place simultaneously. This new approach is able to reproduce the thicknesses of the different mineral facies in the sequence. It has also been successfully applied to model the evolution of the major solutes of the brines trapped as fluid inclusions in halite from the same sequence studied here. The reader is referred to this previous work (Ayora et al., 1994) for a more complete description of the geochemical features and calculations.

### GEOLOGICAL SETTING

The Southpyrenean Eocene Foreland Basin was an east-west elongated trough that was connected to the open sea at its northwestern edge (Fig. 1). The Paleogene sediments infilling the basin show a record of marine (deltas and reefs) to continental (lacustrine and

alluvial) environmental evolution. The transition between marine and continental facies associations occurred in the Upper Eocene when evaporites were deposited (gypsum-anhydrite, halite, and potash facies). Two main evaporite depocenters developed: the Catalonia depocenter at the eastern sector of the foreland and the Navarra depocenter, 300 km to the west (Fig. 1). The Upper Eocene sediments corresponding to the central part of the basin between the two depocenters are covered by the Southpyrenean thrust-sheets, and borehole data in that sector are lacking. However, a connection of the two evaporite depocenters has been suggested by different authors ever since the first hypothesis of Puigdefábregas (1975). The detailed petrographical and geochemical correlation of the evaporite sequences of Catalonia and Navarra has been considered proof that both depocenters belong to a unique evaporite basin (Pueyo, 1975; Rosell, 1983; Busquets et al., 1986).

Evaporites crop out in the basin margins (mainly in the eastern and southeastern sectors of the Catalonia depocenter), where it is possible to determine the vertical and lateral relationships with other related sediments. Above reef carbonates and deltaic marls, sediments crop out showing progressive restriction of the basin: anoxic marls, stromatolites, and evaporites (gypsum and anhydrite). In the margins of the basin the gypsum/anhydrite series averages about 20 m thick. It is formed by secondary gypsum at the surface and anhydrite in buried series. Selenite pseudomorphs are usually preserved in the lower part of the series, while the upper part is made of gypsum breccias and gypsarenites.

The central evaporite series are accessible in mine works and some boreholes for potash exploration. This evaporite sequence is formed by a Mg-sulfate free mineral paragenesis. The sequence is 300 m and 150 m thick at the centers of the Catalonia and Navarra basins, respectively. The borehole of Biurrun, located in the Navarra basin (Fig. 1), was selected for a detailed study due to the following reasons: (1) the continuity of the record of the complete evaporite sequence and (2) the previous available information on lithofacies and geochemical evolution of fluid inclusions throughout the section. Due to its marginal location with respect to the Navarra evaporite depocenter, the sequence is reduced in thickness. The following units from base to top are distinguished (Fig. 2).

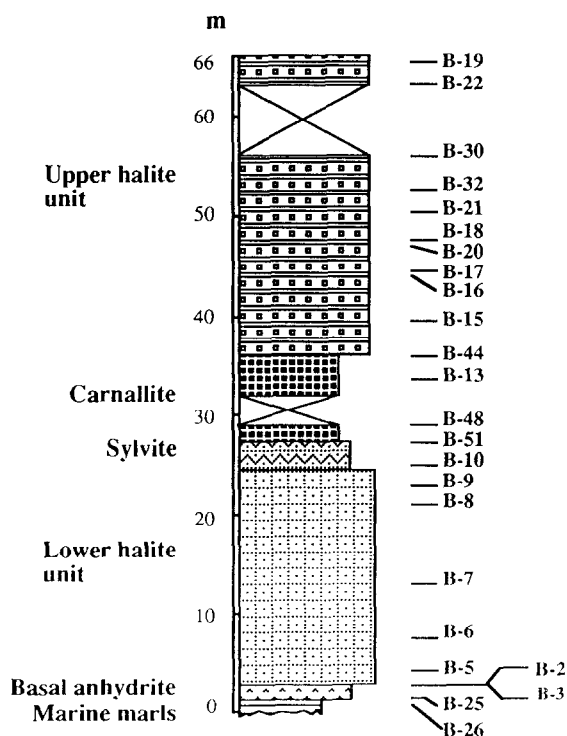


FIG. 2. Stratigraphic sequence cored at Biurrun borehole. The locations of samples in Table 1 are indicated on the right.

- 1) The Basal Anhydrite Unit: It is made up of laminated anhydrite, some 1.3 m thick, located above marine anoxic marls.
- 2) The Lower Halite Unit: It is composed of 20 m of massive coarse-grained halite displaying a banded structure (*sensu* Dellwig, 1955). It is formed by alternating white and dark halite layers (cm thick) with abundant hopper crystals. Minor amounts of anhydrite and polyhalite are found along the grain boundaries of halite distributed throughout the unit.
- 3) The Potash Unit: It is formed by a lower sylvite member and an upper carnallite member. The lower sylvite member is mined for potash. In the Subiza mine, close to Biurrun, the sylvite member is made up of 2 m of alternating centimeter-scale bands of halite and sylvite and millimeter-scale bands of dark clays. Minor amounts of anhydrite also exist. In the Biurrun borehole, however, the sylvite member constitutes 2 m sylvite-cemented halite crystals. Anhydrite is dispersed, or in thin laminae in the halite. The carnallite member is made of about 10 m of alternating beds (tens of centimeters thick) of carnallite and thinner halite, anhydrite and clay horizons. Carnallite is reddish in color, coarse grained, and usually brecciated.
- 4) The Upper Halite Unit: It is constituted by 50 m of alternating halite and clays. The lithofacies is similar to that described for the Potash Unit, but the potash minerals are absent and the clay beds are thicker. Anhydrite laminae are found interbedded with the clay and halite beds. The clay intercalations are reddish in color.

## ANALYTICAL METHODS AND RESULTS

The isotopic composition has been measured in thirty-seven samples of sulfates from the basal anhydrite and those intercalated in other lithofacies throughout the Biurrun borehole. Six further samples of a marginal evaporite series have also been analyzed to provide a marine reference. The marginal evaporite samples have been taken from the Torrent de Calaf section, near the eastern boundary of the basin (Fig. 1). This section comprises 15 m of selenitic gypsum, together with laminated gypsum and gypsarenites. The six samples analyzed were collected systematically throughout the selenitic facies.

Sulfate samples were dissolved in boiling distilled water. The solution was then filtered and  $\text{BaSO}_4$  precipitates were obtained by adding  $\text{BaCl}_2 \cdot 2\text{H}_2\text{O}$  0.2 N, in acid media. The isotopic composition of sulfates has been obtained from the  $\text{BaSO}_4$  precipitates. The oxygen isotopic composition of sulfate has been determined according to the method of Longinelli and Craig (1967), and that of sulfur after that of Filly et al. (1975). The  $\text{CO}_2$  and  $\text{SO}_2$  gas obtained through each method was analysed with a triple collector Sira 9 Isogas mass spectrometer. The results are presented in the classical  $\delta^{18}\text{O}\text{‰}$  SMOW notation for the oxygen and  $\delta^{34}\text{S}\text{‰}$  CDT for the sulfur. Reproducibility of samples and precision, calculated from standards systematically interspersed in the analysed batches, is better than  $\pm 0.1\text{‰}$  for both sulfur and for oxygen.

The result of the analyses are presented in Tables 1 and 2, and are plotted in Fig. 3. The  $\delta$  values are widely scattered, suggesting a record of different geochemical processes. In spite of this variation, some distinct isotopic signatures correspond to particular stages of the evaporite sequence. The marginal sulfates cluster in a distinct area (Fig. 3), corresponding to values of  $+21.9\text{‰} > \delta^{34}\text{S} > +20.8\text{‰}$  and  $+12.9 > \delta^{18}\text{O} > +11.4\text{‰}$ . This cluster agrees with the usually accepted values for marine Tertiary sulfates (Holser and Kaplan, 1966; Claypool et al., 1980) and with the values recorded by Utrilla et al. (1992) among the marine Paleogene sulfates from Spain.

The sulfates from Biurrun borehole show a wide variation of  $\delta$  values. The interpretation of this dispersion is not apparent from Fig. 3. The lowermost part of the Basal Anhydrite Unit show values higher than the marine Tertiary gypsum. The uppermost samples from the basal anhydrite bed ( $+21.3\text{‰} > \delta^{34}\text{S} > +20.8\text{‰}$ ;  $+11.4\text{‰} > \delta^{18}\text{O} > +10.0\text{‰}$ ) are, however, slightly depleted in heavy isotopes relative to the composition of marine Tertiary sulfates. Lower  $\delta$  values are recorded in samples from the Lower Halite and Potash Units ( $+21.3\text{‰} > \delta^{34}\text{S} > +18.1\text{‰}$ ;  $+10.2\text{‰} > \delta^{18}\text{O} > +8.2\text{‰}$ ). Samples of sulfates from the Upper Halite Unit show a wide variation which reaches about 10‰ for the  $\delta^{34}\text{S}$  values and only 2‰ for the  $\delta^{18}\text{O}$

values ( $+23.6\text{‰} > \delta^{34}\text{S} > +12.9\text{‰}$ ;  $+11.9\text{‰} > \delta^{18}\text{O} > +9.8\text{‰}$ ). The lowest  $\delta$  values measured, which correspond to the uppermost part of the Upper Halite Unit, are in agreement with the isotopic composition of Upper Triassic sulfates.

## NUMERICAL MODEL

The geochemical evolution of the evaporite basin was simulated using the conceptual model of a hydrologically open basin proposed by Sanford and Wood (1991). The main principle supporting the calculations is the conservation of the volume of the brine:

$$\frac{dV}{dt} = Q_{\text{SW}} + Q_{\text{RW}} - Q_{\text{L}} - Q_{\text{E}}; \quad (1)$$

and the conservation of the mass of every solute  $i$ :

$$\frac{d(Vc_i)}{dt} = Q_{\text{SW}}c_{\text{SW}} + Q_{\text{RW}}c_{\text{RW}} - Q_{\text{L}}c_i - \sum_{j=1}^{N_M} \nu_{ji} \frac{dm_j}{dt} \quad (2)$$

$i = 1, \dots, N_c$

where  $c_i$  is the concentration (mol/L solution) of the  $i$ th solute in a basin filled with  $V$  liters of water (Fig. 4);  $Q_{\text{SW}}$  and  $Q_{\text{RW}}$  are the water inflows (L/time unit) from the sea and continent (rivers and groundwater);  $Q_{\text{E}}$  is the outflow due to evaporation;  $Q_{\text{L}}$  the outflow due to reflux to the sea or leakage to aquifers;  $dm_j/dt$  is the amount (mol mineral/time unit) of the  $j$ th mineral formed;  $\nu_{ji}$  is the stoichiometric coefficient of the  $i$ th solute in the  $j$ th mineral;  $N_c$  is the number of solutes; and  $N_M$  the number of minerals present in the system. The last term in Eqn. 2 is the total amount of solute (mol/time unit) precipitated in mineral phases. The  $Q_{\text{L}}$  value is a measure of the degree of restriction of the basin to the sea, and ranges from a completely closed system ( $Q_{\text{L}} = 0$ ) to a system completely open to the sea ( $Q_{\text{L}} = Q_{\text{SW}} + Q_{\text{RW}}$ ). The model assumes variable proportions of  $Q_{\text{SW}}$ ,  $Q_{\text{RW}}$ , and  $Q_{\text{L}}$ , whereas the composition of sea and river waters,  $c_{\text{SW}}$  and  $c_{\text{RW}}$ , were considered constant (Table 3). The values of  $c_{\text{SW}}$  were taken from an average of seawater contents (Holland et al., 1986). Instead of a world average of rivers, the values of  $c_{\text{RW}}$  were assumed equal to the solute content of Guadalquivir river, southeastern Spain (MOPU, 1990), due to its recharge area being constituted by carbonates, clays, and evaporites, lithologies similar to those forming the Pyrenean sedimentary cover.

The basin is assumed to have generally evolved with a constant volume of water ( $(Q_{\text{SW}} + Q_{\text{RW}})/(Q_{\text{E}} + Q_{\text{L}}) = 1$ ). Thus, the evaporated volume of water was replaced by an equal volume of seawater or continental water, and complete mixing was assumed. In some particular cases, however, the evolution of the basin has been modeled with the volume of the basin varying continuously ( $(Q_{\text{SW}} + Q_{\text{RW}})/(Q_{\text{E}} + Q_{\text{L}}) = A \neq 1$ ;  $\Delta V/V = (1 - A) \times \text{number of basins evaporated}$ ).

The thermodynamics of chemical equilibrium is used to calculate the molar quantities of precipitating phases, and the concentration of every solute in the brine. Thus, a system of  $N_c$  mass balance equations and  $N_M$  mass action law equations can be established (Crerar, 1975). Details of the numerical solution of the equations can be found in Ayora et al. (1994). The model describing the thermodynamic behavior of ions in highly concentrated brines is based on the Pitzer ion-ion interaction model. The thermodynamic parameters and the mineral saturation constants at 25°C were taken from Harvie et al. (1984).

The molar amounts of mineral precipitated are transformed into meters of sediment per unit of surface using the molar volume of minerals. In order to compare with the stratigraphical record, porosity was assumed to be zero. The calculations are normalized for 1 m depth of water. The thickness of sediment deposited is directly obtained by multiplying the result of the calculation by the depth of the brine (in meters) assumed in the basin. This depth represents the water directly involved in the evaporation/precipitation process and is called here the effective depth. The real depth of water in the basin may be either equal or higher and it cannot be inferred directly from the model.

The  $\delta^{18}\text{O}_{\text{B}}$  and  $\delta^{34}\text{S}_{\text{B}}$  values of the sulfate in the brine were calculated using the mass balance constraints of Eqns. 1 and 2:

Table 1. Isotopic composition values of sulfates from Biurrun borehole. The location of the sample in the borehole has been represented as meters below the surface. The real thickness of the evaporite sequence has been obtained after subtracting the thickness of clastics. The samples have also been located with respect to the real thickness from the bottom of the sequence.

| Evaporite unit   | Sample | Depth (m) | Real thickness (m) | $\delta^{34}\text{S}\text{‰ CDT}$ | $\delta^{18}\text{O}\text{‰ SMOW}$ |
|------------------|--------|-----------|--------------------|-----------------------------------|------------------------------------|
| Upper halite     | 19     | -375,50   | 49,25              | +12,95                            | +11,60                             |
|                  | 22     | -378,00   | 47,85              | +13,55                            | +10,91                             |
|                  | 30     | -385,00   | 45,35              | +14,54                            | +11,04                             |
|                  | 32     | -387,67   | 43,90              | +14,92                            | +11,38                             |
|                  | 21     | -390,00   | 42,55              | +14,88                            | +11,11                             |
|                  | 18     | -392,80   | 40,65              | +15,21                            | +11,17                             |
|                  | 20     | -393,40   | 38,95              | +15,38                            | +10,95                             |
|                  | 17     | -395,70   | 37,25              | +14,76                            | +10,97                             |
|                  | 16     | -397,00   | 36,50              | +17,29                            | +11,28                             |
|                  | 38     | -398,70   | 35,45              | +18,08                            | +11,87                             |
|                  | 39     | -399,75   | 34,80              | +18,00                            | +10,26                             |
|                  | 40     | -400,85   | 34,00              | +19,13                            | +11,43                             |
|                  | 15     | -402,50   | 33,60              | +19,27                            | +9,88                              |
|                  | 41     | -403,47   | 32,30              | +23,55                            | +11,66                             |
|                  |        |           |                    |                                   |                                    |
| Carnallite       | 44     | -404,90   | 32,15              | +19,39                            | +8,48                              |
|                  | 14     | -405,00   | 32,00              | +18,17                            | +8,53                              |
|                  | 46     | -405,45   | 31,90              | +21,31                            | +10,16                             |
|                  | 13     | -407,80   | 30,20              | +18,12                            | +9,39                              |
|                  | 48     | -412,63   | 26,30              | +20,15                            | +9,20                              |
|                  | 49     | -413,27   | 25,60              | +20,01                            | +8,36                              |
| Sylvite          | 51     | -413,80   | 25,10              | +20,68                            | +8,23                              |
|                  | 12     | -414,00   | 24,90              | +19,66                            | +9,07                              |
|                  | 23     | -414,20   | 24,70              | +19,58                            | +8,51                              |
|                  | 11     | -415,00   | 23,90              | +19,86                            | +8,77                              |
|                  | 52     | -415,35   | 23,50              | +21,19                            | +9,16                              |
| Lower halite     | 10     | -416,00   | 22,90              | +20,93                            | +9,50                              |
|                  | 9      | -417,50   | 21,40              | +20,26                            | +9,65                              |
|                  | 8      | -419,30   | 19,60              | +20,07                            | +9,56                              |
|                  | 7      | -427,50   | 11,40              | +20,24                            | +9,44                              |
|                  | 6      | -433,00   | 5,90               | +20,24                            | +9,35                              |
|                  | 5      | -436,20   | 2,70               | +19,97                            | +9,21                              |
| Basal anhydritic | 2      | -437,50   | 1,40               | +20,80                            | +11,43                             |
|                  | 1      | -437,51   | 1,39               | +21,25                            | +10,87                             |
|                  | 4      | -437,52   | 1,38               | +21,15                            | +10,05                             |
|                  | 3      | -437,53   | 1,37               | +20,90                            | +11,36                             |
|                  | 24     | -438,30   | 0,60               | +23,69                            | +13,04                             |
|                  | 25     | -438,90   | 0,10               | +23,14                            | +13,24                             |

$$\frac{d(Vc_B\delta^{34}S_B)}{dt} = Q_{SW} \cdot c_{SW}\delta^{34}S_{SW} + Q_{RW}c_{RW}\delta^{34}S_{RW}$$
$$- Q_Lc_B\delta^{34}S_B - \sum_{j=1}^{N_m} \nu_j \frac{d(m_j\delta^{34}S_j)}{dt}, \quad (3)$$

where  $c_{SW}$ ,  $c_{RW}$ , and  $c_B$  are the sulfate concentrations (mol/L), and  $\delta^{34}S_{SW}$ ,  $\delta^{34}S_{RW}$ , and  $\delta^{34}S_B$  are the isotopic composition of sulfate in

the seawater, the continental water, and the basinal brine, respectively;  $dm/dt$  are the molar amounts of the  $j$ th mineral formed,  $\nu_j$  is the stoichiometric coefficient of  $\text{SO}_4$  in the  $j$ th mineral, and  $\delta^{34}S_j$  is the isotopic composition of the  $j$ th mineral. An analogous equation can be made for  $\delta^{18}\text{O}$  values. The  $\delta^{34}S_j$  and  $\delta^{18}\text{O}_j$  values of the mineral are explicitly calculated from the  $\delta^{34}S_B$  and  $\delta^{18}\text{O}_B$  values and the enrichment factors of  $\Delta^{34}S_{\text{min-B}}$  and  $\Delta^{18}\text{O}_{\text{min-B}}$  of +1.65 and +3.5, respectively (Thode and Monster, 1965; Lloyd, 1968).

DISCUSSION OF RESULTS

The Isotopic Composition of Upper Eocene Marine Sulfates

The isotopic composition of the samples from the marginal sulfates (selenitic facies) plots in a well-constrained group with average values of  $\delta^{34}\text{S} = +21.6 \pm 0.4\text{‰}$  and  $\delta^{18}\text{O} \approx +12.2 \pm 0.6\text{‰}$  ( $\pm 1\sigma$ ). These values are within the estimated range of variation of the Upper Eocene marine sulfates presented in the isotope age curves by Claypool et al. (1980). However, the values from the marginal sulfates hereby discussed are slightly heavier than the  $\delta^{34}\text{S}$  values from Eocene evaporite samples analyzed by Thode and Monster (1965)

Table 2. Isotopic composition values of selenites from the Torrent de Calaf section.

| Sample | $\delta^{34}\text{S}\text{‰ CDT}$ | $\delta^{18}\text{O}\text{‰ SMOW}$ |
|--------|-----------------------------------|------------------------------------|
| TC-10A | +21,66                            | +11,48                             |
| TC-9B  | +21,88                            | +12,43                             |
| TC-7B  | +21,94                            | +12,92                             |
| TC-7A  | +21,55                            | +12,76                             |
| TC-8B  | +21,62                            | +11,40                             |
| TC-6H  | +20,85                            | +12,00                             |

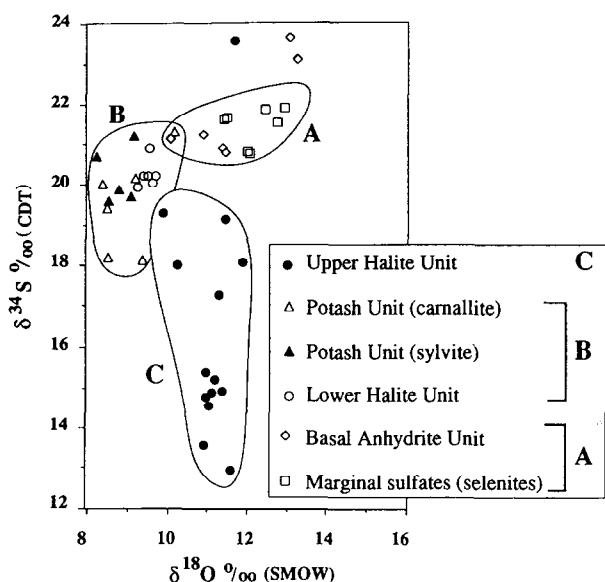


FIG. 3. Plot of the isotopic composition of sulfates from the Biurrun borehole and the Torrent de Calaf section.

[+18.4 to +22.1] and Claypool et al. (1980) (+10.9 to +19.9, with an extreme value of +25.5). Regarding oxygen, the marginal sulfates from the Torrent de Calaf section display  $\delta$  values lower than the best estimated values (about +14‰) for the oxygen isotope age curve presented by Claypool et al. (1980). The isotopic composition dataset for middle and upper Eocene sulfate has been recently improved by Utrilla et al. (1992) with samples from the southern Pyrenean foreland. Their results give average values of  $\delta^{34}\text{S} = +21.4 \pm 0.4\text{‰}$  and  $\delta^{18}\text{O} = +12.6 \pm 0.9\text{‰}$  for Middle Eocene evaporites and  $\delta^{34}\text{S} = +21.5 \pm 1.2\text{‰}$  and  $\delta^{18}\text{O} = +11.7 \pm 1.0\text{‰}$  for Upper Eocene evaporites. This range of values is in good agreement with those for the marginal sulfates from the Torrent de Calaf section. Therefore, the mean  $\delta^{34}\text{S}$  and  $\delta^{18}\text{O}$  values for marginal sulfates analyzed in the present study have been used to calculate a representative isotopic composition of the sulfate dissolved in the Upper Eocene seawater:  $\delta^{34}\text{S} = +20.0\text{‰}$  and  $\delta^{18}\text{O} = +8.7\text{‰}$ .

### Sulfate Isotopic Composition During Basin Restriction

#### Basal Anhydrite Unit

In order to simulate the formation of the Basal Anhydrite Unit, an initial solution with the composition of seawater was evaporated with seawater replacing the evaporated water ( $Q_{\text{SW}} = Q_{\text{E}} + Q_{\text{L}}$ ;  $Q_{\text{RW}} = 0$ ). A certain restriction of the basin is required for evaporite minerals to form. According to solubility calculations first carbonates, followed by gypsum, anhydrite, and finally halite are predicted to precipitate as evaporation progresses. However, in a completely restricted basin ( $Q_{\text{L}}/Q_{\text{E}} = 0$ ) unrealistically low amounts of each mineral precipitate previous to the next soluble mineral. It appears that the evaporation of seawater in the described open basin with  $Q_{\text{L}}/Q_{\text{E}}$  values close to 0.13 is the most reliable mechanism to form the 1.3 meter-thick anhydrite layer observed in the Biurrun sequence. With this restriction value the basin reaches the

steady state composition and sufficient amounts of anhydrite (and minor carbonate) precipitate. Higher  $Q_{\text{L}}/Q_{\text{E}}$  values lead to carbonate + gypsum or carbonate as the only minerals to form, whereas lower  $Q_{\text{L}}/Q_{\text{E}}$  values lead to the formation of halite when only minor amount of anhydrite is formed.

As a result of evaporation in the above described scenario, the evolution of the calculated  $\delta^{34}\text{S}$  and  $\delta^{18}\text{O}$  values of anhydrite is controlled by the composition of seawater sulfate (Fig. 5). The two lower samples of the Basal Anhydrite Unit, however, display  $\delta^{34}\text{S}$  and  $\delta^{18}\text{O}$  values higher than predicted. Bacterial sulfate reduction processes taking place on the bottom of the basin may account for such isotopic enrichments. Thus, the ratios of enrichment ( $\Delta^{34}\text{S}/\Delta^{18}\text{O}$ ) of these two samples with respect to the average of isotopic composition of the marginal evaporites are 1.5 and 2.5. These values are included in the range of enrichment ratios found for bacterial reduction processes in laboratory and natural environments (Rafter and Mizutani, 1967; Mizutani and Rafter, 1973). Another alternative explanation for the heavy  $\delta^{34}\text{S}$  and  $\delta^{18}\text{O}$  values of the two lower samples of the Basal Anhydrite Unit would be that the isotopic composition of seawater sulfate was higher than assumed. This hypothesis, however, would lead to  $\delta$  values of the precipitates being unrealistically high compared with the  $\delta$  values of sulfates from the entire sequence at the margins and evaporite depocenter.

#### The Lower Halite Unit

The continuation of the evaporation process described above would lead to the indefinite deposition of anhydrite. Hence, a change in the hydrological conditions of the basin, i.e., an increase of the restriction degree ( $Q_{\text{L}}/Q_{\text{E}} < 0.13$ ), is required to precipitate the Lower Halite Unit. To simulate such a process an initial brine with the composition equal to that resulting from the precipitation of anhydrite was evaporated with seawater flowing into the basin in order to keep the total volume constant ( $Q_{\text{SW}}/(Q_{\text{E}} + Q_{\text{L}}) = 1$ ;  $Q_{\text{RW}}/(Q_{\text{E}} + Q_{\text{L}}) = 0$ ). The following mineral sequence is then predicted: car-

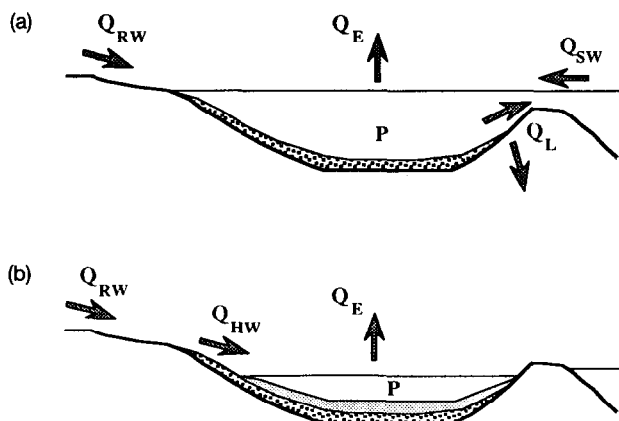


FIG. 4. Conceptual model of the input and output flows in an hydrologically open evaporite basin: (a) Open to the sea (Basal Anhydrite and Lower Halite Units), (b) Endorheic (Potash and Upper Halite Units). Legend:  $Q_{\text{SW}}$  = seawater inflow;  $Q_{\text{RW}}$  = continental water inflow;  $Q_{\text{L}}$  = outflow by reflux and leakage to aquifers;  $Q_{\text{E}}$  = evaporation outflow.

bonates + anhydrite + halite, and later polyhalite, which is consistent with that observed in the Lower Halite Unit. In order to explain the sulfate depletion measured in fluid inclusions and the subsequent formation of sylvite instead of Mg-sulfates, a small amount of a hypothetical  $\text{CaCl}_2$ -rich brine has also been assumed to flow into the basin.

As explained in detail in Ayora et al. (1994), values of  $Q_L/Q_E$  between 0.1 and 0.02 lead to the precipitation of halite + anhydrite + carbonates in a steady state brine composition. Values of  $Q_L/Q_E$  lower than 0.02 lead to the precipitation of the observed thickness of the Lower Halite Unit previous to sylvite only if an effective depth of water of 25 m is assumed in the basin. Values of  $Q_L/Q_E$  decreasing from 0.1 to 0.0, as expected from the reduction in porosity of the sediments on the bottom of the basin, are also possible. Therefore, values of  $Q_L/Q_E$  ranging from 0.1 to 0.0 give similar mineral associations.

The calculated evolution of the  $\delta^{34}\text{S}$  and  $\delta^{18}\text{O}$  values under the conditions described above is very similar regardless of the value of  $Q_L/Q_E$  (Fig. 5). The increase in the degree of restriction leads to the precipitation of anhydrite, not compensated by the recharge, and to a drop in the calculated  $\delta^{34}\text{S}$  and  $\delta^{18}\text{O}$  values (limited reservoir effect). This effect is well recorded in the four samples from the uppermost five centimeters of the Basal Anhydrite Unit. The ratios of enrichment ( $\Delta^{34}\text{S}/\Delta^{18}\text{O}$ ) of the four samples with respect to the average isotopic composition of marginal sulfates plot very close to +0.45. This value is coincident with that theoretically calculated (+0.47) for crystallization with the enrichment factors used here ( $\Delta^{34}\text{S}_{\text{mineral-SO}_4} = +1.65\text{‰}$ ;  $\Delta^{18}\text{O}_{\text{mineral-SO}_4} = +3.50\text{‰}$ ), and confirms that the observed trend in the  $\delta^{34}\text{S}$  and  $\delta^{18}\text{O}$  values may be due to mineral crystallization.

Once the new restriction conditions are established the precipitated amount of sulfate is compensated by the seawater inflow and its concentration in the brine reaches a steady state (Table 3). This trend is clearly different from that calculated in closed systems where the  $\delta^{34}\text{S}$  and  $\delta^{18}\text{O}$  values decrease continuously as evaporation progresses. Developing Eqn. 3 with constant volume and the steady state condition for the isotopic composition the following expression is obtained:

$$\delta^{34}\text{S}_B = \frac{Q_{\text{SW}}c_{\text{SW}}(\delta^{34}\text{S}_{\text{SW}} - \Delta) + Q_{\text{RW}}c_{\text{RW}}(\delta^{34}\text{S}_{\text{RW}} - \Delta) - Q_Lc_B\Delta}{Q_{\text{SW}}c_{\text{SW}} + Q_{\text{RW}}c_{\text{RW}}}, \quad (4)$$

where  $\Delta$  is the sulfur enrichment value, which is assumed to be a constant value ( $\Delta$ ) through evaporation and equal for all the sulfates precipitated. A similar expression can be obtained

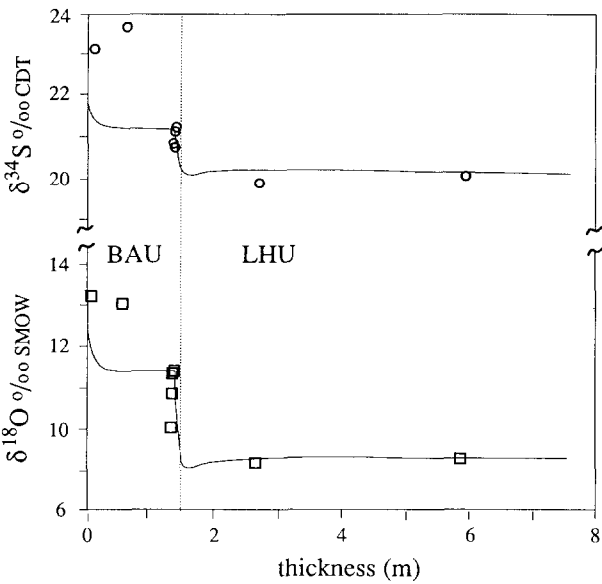


FIG. 5. Evolution of the calculated isotopic composition of precipitated sulfate with respect to the thickness of the Basal Anhydrite Unit (BAU) and the lowermost part of the Lower Halite Unit (LHU). Hydrological parameters used in the simulations: (a)  $Q_{\text{SW}}/(Q_{\text{SW}} + Q_{\text{RW}}) = 1$ ,  $Q_{\text{RW}}/(Q_{\text{SW}} + Q_{\text{RW}}) = 0$ ,  $Q_L/Q_E = 0.13$ ; (b)  $Q_{\text{SW}}/(Q_{\text{SW}} + Q_{\text{RW}}) = 0.8$ ,  $Q_{\text{RW}}/(Q_{\text{SW}} + Q_{\text{RW}}) = 0.2$ ,  $Q_L/Q_E = 0.13$ .

for the  $\delta^{18}\text{O}_B$  value. As pointed out above, values of  $Q_L/Q_E$  between 0.1 and 0.02 lead to the formation of the Lower Halite Unit in a steady state brine composition and the condition for isotopic composition is also fulfilled (Fig. 5). However, the Lower Halite Unit can also be formed under conditions of no steady state ( $Q_L/Q_E < 0.02$ ). On such case the value of  $c_B$  and the rate of precipitation of sulfates (anhydrite and then polyhalite) are not constant. The influence of these changes in the  $\delta^{34}\text{S}_B$  and  $\delta^{18}\text{O}_B$  values, however, is very small and the isotopic composition reaches a quasi-steady state (Fig. 5). Hence, the isotopic composition of the sulfates found throughout the Lower Halite Unit can be explained by seawater evaporation with a moderate to high degree of restriction ( $Q_L/Q_E = 0.1$  to  $0$ ).

Seawater has been assumed to be the only recharge in the above discussion. Evaporation processes with minor proportions of continental inflow would also lead to the formation of mineral associations similar to those observed. However, as the sulfate concentration in seawater ( $c_{\text{SW}}$ ) is one order of magnitude higher than that of river water ( $c_{\text{RW}}$ ), the influence

Table 3.- Composition of inflow water used in the calculations (in mmol/kg): SW) Average of the oceans (Holland et al., 1986); RW) river Guadalentin (M.O.P.U., 1990); HW) River water saturated in halite. Isotopic composition of sulfate dissolved in inflow water calculated from: SW) Mean of analyses of Upper Eocene selenites from the margins of the evaporite basin minus the isotopic enrichment factor; RW) Mean of analyses of Upper Triassic sulfates from Southern Pyrenees and Iberian Peninsula (Utrilla et al., 1992); HW) Mean of analyses of sulfates intercalated in the Lower Halite Unit.

|    | Na                  | K    | Mg   | Ca   | Cl                  | SO <sub>4</sub> | HCO <sub>3</sub> | δ <sup>34</sup> S | δ <sup>18</sup> O |
|----|---------------------|------|------|------|---------------------|-----------------|------------------|-------------------|-------------------|
| SW | 468.0               | 10.2 | 53.2 | 10.2 | 545.0               | 28.2            | 2.4              | 20.0              | 8.7               |
| RW | 15.8                | 0.5  | 5.7  | 5.5  | 13.6                | 5.4             | 1.8              | 13.5              | 11.8              |
| HW | 5.9x10 <sup>3</sup> | 0.5  | 5.7  | 5.5  | 6.0x10 <sup>3</sup> | 5.4             | 1.8              | 20.3              | 9.5               |

of continental sulfate in the  $\delta^{34}\text{S}_\text{B}$  and  $\delta^{18}\text{O}_\text{B}$  values is not significant and has not been considered.

### Sulfate Isotopic Composition in Highly Evaporated Facies

Continuing the evaporation under the same conditions that formed the Lower Halite Unit, with low or decreasing  $Q_\text{L}/Q_\text{E}$  values, would yield the formation of sylvite and then carnallite, together with halite, anhydrite, polyhalite, and carbonates. However, several sedimentological features indicate that a dramatic change in the hydrology of the basin took place at this stage. The noticeable shrinkage of the area occupied by the Potash Unit compared with that of the Lower Halite Unit in both Catalonia and Navarra depocenters points to an important reduction in the volume of water in the basin. Drastic reduction in volume of water can only be achieved if the basin closes, totally or partially, to seawater recharge. The increasing amount of clastics at the top of the Upper Halite Unit and the general reddening of the sequence suggest the relative increasing importance of continental recharge. The type of sedimentation changed from massive halite to rhythmic interbedding of evaporites and clastics, confirming the cyclic character of the recharge. Therefore, the basin shallowed until the air-brine surface was sufficiently small for evaporation to be only compensated by the recharge. Moreover, the proportions of contemporaneous sylvite/halite and camallite/halite observed in the Biurrun borehole and in the mining works of both the Catalonia and Navarra depocenters is always close to 1/1 and 10/1, respectively. Such proportions are obtained from the evaporation process referred to above with no seawater inflow and, as discussed in detail in Ayora et al. (1994), higher values of  $Q_\text{SW}$  lead to mineral proportions richer in halite than observed.

In order to examine the variation of the sulfate isotopic composition during evaporation under the recharge constraints described above, an initial brine with a solute concentration close to that precipitating the Lower Halite Unit was evaporated in two different continental recharge/evaporation ratios: no recharge and  $Q_\text{RW} = 0.5$ . In both cases the following succession of parageneses result from the calculations: halite + anhydrite + (polyhalite) + carbonates, then sylvite + halite + anhydrite + (polyhalite) + carbonates, and then camallite + halite + anhydrite + (polyhalite) + carbonates. This succession and the relative proportions of minerals match those observed in the Biurrun borehole and the potash deposits mined in the region. The basin was assumed to be completely restricted ( $Q_\text{L}/Q_\text{E} = 0$ ) in both cases. Since kieserite and bischoffite have never been described in the area, the evaporation was stopped before the Mg-sulfates formation was reached. This is equivalent to a reduction of 80% of the initial volume of the basin ( $\Delta V/V = -0.8$ ). As already pointed out in the description of the numerical model, the calculated thickness of mineral deposits also depends on the effective depth of water assumed in the basin. The average depth of water was arbitrarily fixed to form 9 meters of Potash Unit (the thickness intersected by the Biurrun borehole).

The evolution of the isotopic composition of sulfates formed in the two different evaporation conditions show a similar decrease in the  $\delta^{34}\text{S}$  and  $\delta^{18}\text{O}$  values due to the precipitation of sulfates not compensated by an equivalent inflow

of sulfate (limited reservoir effect). Since the volume is not held constant a new steady state is not expected. Some of the  $\delta^{34}\text{S}$  values and, particularly those of  $\delta^{18}\text{O}$  (due to the larger fractionation factor of oxygen), clearly show the limited reservoir effect (Fig. 6) and confirm the evaporation conditions previously assumed.

The remainder of the analyses, however, do not match the calculated trend and deserve further discussion. The analyses with  $\delta^{34}\text{S}$  and  $\delta^{18}\text{O}$  values higher than predicted can only be explained if a new recharge with high  $\delta^{34}\text{S}$  and  $\delta^{18}\text{O}$  values flows into the system. Due to the decreasing level of water in the basin, part of the already formed evaporites (mainly the Lower Halite Unit) could result exposed to dissolution and recycling by ground and surface waters. A new inflow  $Q_\text{HW}$  with the  $\delta^{34}\text{S}$  and  $\delta^{18}\text{O}$  values for the sulfates interbedded in the Lower Halite Unit has been considered (Table 3). The  $\delta$  values of this recharge, together with the effect of enrichment during mineral precipitation, may account for the  $\delta^{34}\text{S}$  and  $\delta^{18}\text{O}$  values observed in some samples. On the other hand, as will be discussed for the Upper Halite Unit, the analyses with  $\delta^{34}\text{S}$  and  $\delta^{18}\text{O}$  values, respectively, lower and higher than predicted, found at the top of the Potash Unit, can only be explained by an important inflow of river water  $Q_\text{RW}$  with sulfate of Triassic signature (Table 3). Tentative calculations have been unsuccessful in modeling accurately the dispersion of the  $\delta$  values analyzed, probably due to the oversimplifications made in the theoretical model. Thus, the assumption of complete mixing and compositional homogeneity is not realistic for highly evaporated brines as proved by experiments and observations in nature (Sonnenfeld, 1984).

### Sulfate Isotopic Composition Resulting from Recycling Older Evaporites

As described in detail in Ayora et al. (1994) the dilution of the residual brine by the increase in the proportion of the continental recharge accounts for the end of camallite precipitation and for the solute proportions of the fluid inclusions from the base of the Upper Halite Unit. Once the dilution is achieved, the Upper Halite Unit can be formed by evaporation of the brine with continental recharge replacing an equal evaporated volume. However, the proportion of the two continental inflows,  $Q_\text{RW}$  and  $Q_\text{HW}$ , are not constrained by the parageneses and the fluid inclusion composition.

The uppermost anhydrite samples show  $\delta^{34}\text{S}$  and  $\delta^{18}\text{O}$  values close to the isotopic composition of Upper Triassic sulfates (Table 3). The Triassic source has already been pointed out for the sulfate from other localities in the Ebro basin (Birnbbaum and Coleman, 1979; Utrilla et al., 1992). The rest of samples from the Upper Halite Unit show  $\delta^{34}\text{S}$  and  $\delta^{18}\text{O}$  values to plot between the Upper Triassic sulfates and those recorded for the Eocene sulfates from the margins of the basin and from the Lower Halite Unit (Table 3). This is specially evident in the case of sulfur where the difference in the extreme  $\delta^{34}\text{S}$  values reaches 9‰. Assuming an Upper Triassic isotopic signature for the sulfate in the river water inflow ( $Q_\text{RW}$ ), and that of sulfate in the Lower Halite Unit for the recycling inflow ( $Q_\text{HW}$ ), the isotopic composition of the anhydrite intercalated in the Upper Halite Unit may give some indication on the relative proportions of the recharge.

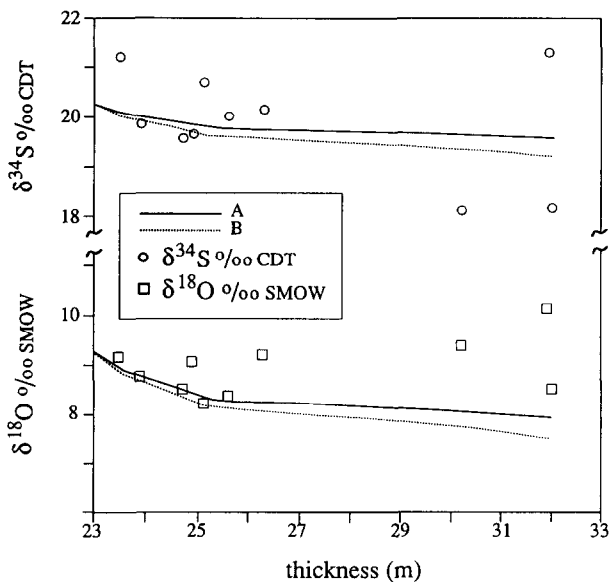


FIG. 6. Evolution of the calculated isotopic composition of precipitated sulfate with respect to thickness (clastics excluded) corresponding to the formation of the Potash Unit. Hydrological parameters used in the simulations: (a)  $Q_{RW}/Q_E = 0$ ,  $Q_{HW}/Q_E = 0$ ; (b)  $Q_{RW}/Q_E = 0.5$ ,  $Q_{HW}/Q_E = 0$ .  $Q_L = 0$ , and  $Q_{SW} = 0$  assumed for all the calculations.

Unfortunately, the slope of the calculated trend of the  $\delta^{34}\text{S}$  and  $\delta^{18}\text{O}$  values with respect to the thickness of the sequence depends on many unconstrained parameters and cannot be successfully modeled. However, some of these uncertainties can be overcome if steady state for the  $\delta^{34}\text{S}$  and  $\delta^{18}\text{O}$  values, such as that observed in the uppermost half of the Upper Halite Unit, is reached (Table 3). According to Eqn. 4, the  $\delta^{34}\text{S}_B$  and  $\delta^{18}\text{O}_B$  values for the brine are mainly dependent on the proportion of the sulfate masses in the recharge, in this case ( $Q_{RW} \cdot c_{RW}$ ) and ( $Q_{HW} \cdot c_{HW}$ ). This is evidenced by the calculated trends in Fig. 7, where those corresponding to values of  $Q_{RW} = 0.8$  and  $Q_{HW} = 0.2$  match the analyses from the uppermost half of the Upper Halite Unit. As a first approximation, equal values for  $c_{RW}$  and  $c_{HW}$  have been assumed in the calculations (Table 3). Since a higher amount of sulfate is expected in the water from the Eocene-recycling recharge, the calculated  $Q_{HW}$  value of 0.2 must be considered a maximum value for this inflow.

As expected from Eqn. 4 uncertainties in the initial  $\delta^{34}\text{S}$  and  $\delta^{18}\text{O}$  values are not involved in the calculations at steady state. Moreover, the effective depth of water and the thickness of sequence accumulated may change the slope of the  $\delta^{34}\text{S}$  and  $\delta^{18}\text{O}$  vs. thickness plots in transient states, but has no influence under steady state conditions. On the other hand, variations in the isotopic composition of the Upper Triassic sulfate may also have some effect on the calculation of the  $Q_{RW}$  and  $Q_{HW}$  proportions. Calculations taking into account the statistical variability ( $\pm 1\sigma$ ) in the Upper Triassic sulfate composition from the Pyrenees and Iberian Peninsula enlarge the range of uncertainty in the inferred  $Q_{RW}$  values from approximately 0.7 to approximately 0.9. The  $\delta^{34}\text{S}$  values of the two uppermost samples of the sequence plot outside the range of variability and indicate that an increase in the  $Q_{RW}$  could have taken place at that time.

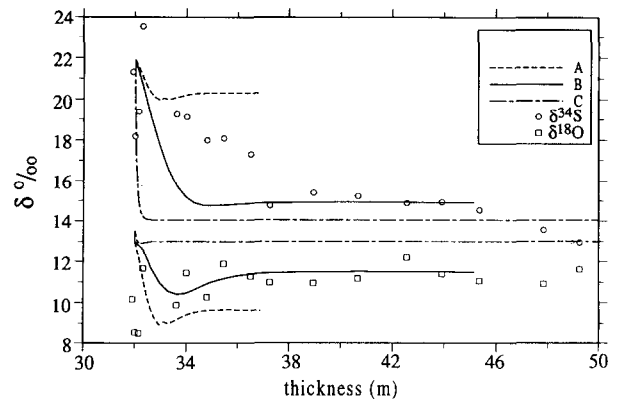


FIG. 7. Evolution of the isotopic composition of precipitated sulfate with respect to thickness (clastics excluded) corresponding to three different proportions of recharge for the formation of the Upper Halite Unit. Initial  $\delta^{34}\text{S}$  and  $\delta^{18}\text{O}$  values equal to those of the Eocene-recycling isotopic composition and an effective depth of water of 10 meters have been assumed. Hydrological parameters used in the simulations: (a)  $Q_{RW}/Q_E = 0$ ,  $Q_{HW}/Q_E = 1$ ; (b)  $Q_{RW}/Q_E = 0.8$ ,  $Q_{HW}/Q_E = 0.2$ ; (c)  $Q_{RW}/Q_E = 1$ ,  $Q_{HW}/Q_E = 0$ .  $Q_L = 0$  and  $Q_{SW} = 0$  assumed for all the calculations. Evolution under option (c) does not form sufficient sequence thickness but imaginary  $\delta^{34}\text{S}$  and  $\delta^{18}\text{O}$  trends have been represented as a reference.

## CONCLUSIONS

The conclusions arising from this study refer to the hydrological regime of the basin at the stage of evaporite formation. Moreover, general conclusions with implications for the evolution of other evaporite basins and for the isotope geochemistry of sulfates have also arisen.

Two main stages, marine and continental, have been distinguished in the development of the studied basin. Both stages have been outlined by the isotopic record which has

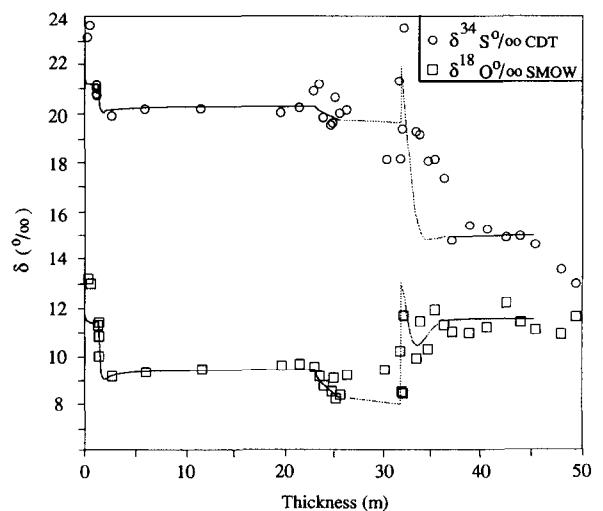


FIG. 8. Plot of analyzed values and calculated evolution of the isotopic composition of precipitated sulfate with respect to the thickness of the Biurrun borehole (clastics excluded). The evaporation conditions are described in the text. The dotted line represent the calculations for a process of dilution of the brine residual from potash formation by a sudden inflow of Eocene-recycling water, it is not constrained and is plotted as an example.



added conclusive information to that obtained from mineral parageneses, particularly in the segments of the sequence where the  $\delta^{34}\text{S}$  and  $\delta^{18}\text{O}$  values remain constant (Fig. 8). The first stage corresponds to the formation of the Basal Anhydrite and Lower Halite units. The mineral sequence corresponds to the evaporation in a basin with a progressive degree of restriction, and evaporation compensated by equal inflow of major marine origin. The  $\delta^{34}\text{S}$  and  $\delta^{18}\text{O}$  values of the two lowermost samples from the Basal Anhydrite Unit can only be explained if bacterial sulfate reduction is assumed. The sharp decrease in the  $\delta^{34}\text{S}$  and particularly the  $\delta^{18}\text{O}$  values recorded at the end of the Basal Anhydrite Unit illustrate a limited reservoir effect produced by the increase of restriction leading to the precipitation of halite. Assuming that in a basin open to the sea the continental inflow represents a minor portion of the recharge, the constant  $\delta^{34}\text{S}$  and  $\delta^{18}\text{O}$  values measured in the sulfates through the Lower Halite Unit are consistent with the isotope composition of upper Eocene seawater calculated from the values of the marginal gypsum.

The second stage of the basin evolution corresponds to the formation of the Potash Unit and the Upper Halite Unit. This stage developed after disconnection of the basin from the sea. The samples intercalated in the sylvite show  $\delta^{34}\text{S}$  and  $\delta^{18}\text{O}$  values to sharply decrease (limited reservoir effect), consistent with evaporation occurring during decreasing volume of water. The variability of the isotopic values of the rest of sulfates intercalated in the Potash Unit has not been successfully modeled. Nevertheless, they suggest the influence of the recycling of both Upper Eocene and Upper Triassic sulfates. The dilution of the residual brine by continental recharge stunts the formation of camallite. The isotope composition of the sulfates from the Upper Halite Unit is consistent with a basin evolving under an endorheic regime with both upper Eocene and upper Triassic-recycling recharges compensating evaporation. Since the  $\delta^{34}\text{S}$  and  $\delta^{18}\text{O}$  values from the uppermost half of the unit indicate that a steady state was reached, an approximate proportion of 80% (total mass of sulfate) of Upper Triassic-recycling source and 20% of Eocene-recycling source is inferred. This steady state clearly indicates that an hypersaline lake with constant volume of brine was established.

Taking into account that the basin evolves towards a progressive increase in the degree of restriction, the  $\delta^{34}\text{S}$  and  $\delta^{18}\text{O}$  values of the selenitic facies of the margins, higher than those of the rest of the described sequence, indicate that the precipitation of the marginal sulfates preceded that of the basal anhydrite in the depocenter.

The present study has also led to conclusions on the isotope geochemistry of sulfates from evaporitic sequences in a much broader scope than the studied basin. To date the reservoir effect of Rayleigh-type has usually been considered to explain the variation of  $\delta^{34}\text{S}$  values of sulfates in evaporitic sequences (e.g., Holser and Kaplan, 1966; Nielsen, 1978; Claypool et al., 1980). The data of the present study are not adequately described by such a closed-system model. The model hereby presented is based on a more realistic hypothesis of an open basin. Hence, the model considers a variable recharge flowing contemporaneously with evaporation, and it is able to predict the observed thickness of sediments and incorporates the effect of the recycling of older evaporites.

The determination of  $\delta^{34}\text{S}$  has to date deserved most of the attention in the isotopic studies of sulfates. More recently, it has also been recognized that coupling both the  $\delta^{34}\text{S}$  and  $\delta^{18}\text{O}$  values will noticeably improve the quantification of processes affecting evaporite basins and at a much larger scale the sulfur cycle (Krouse, 1980; Longinelli, 1989; Holt and Kumar, 1991). It has been evidenced in this study that, due to the larger fractionation factor of oxygen, the  $\delta^{18}\text{O}$  values are more useful in describing processes involving sulfate crystallization. Moreover, due to the different behavior of sulfur and oxygen, the  $\delta^{18}\text{O}$  values may also become important in confirming processes of bacterial sulfate reduction.

The variation in the isotopic composition of sulfates throughout the entire evaporite sequence has been modeled applying the fractionation factors proposed by Thode and Monster (1965) for sulfur and Lloyd (1968) for oxygen. The good agreement between the calculations and the measured values throughout the Lower Halite Unit confirms (within the range of the analytical error) the validity of these fractionation factors for anhydrite and polyhalite. Furthermore, according to our data from the Lower Halite Unit and from the lower part of the Potash Unit, there is no need to assume a change in the fractionation factor of sulfur and oxygen, such as proposed for sulfur by Raab and Spiro (1991), during the precipitation of sulfates of highly evaporated facies.

In the sequences strongly conditioned by the marine inflow, the evolution of the  $\delta^{34}\text{S}$  and  $\delta^{18}\text{O}$  values calculated by the model are based on hypothetical values for seawater recharge. Therefore, the required agreement between the calculated and analyzed values may also constrain the isotopic composition of the oceanic sulfate for a particular age. Hence, an accurate identification of the different processes involved in the formation of a particular sequence and a measurement of the degree of restriction of the basin with respect to the sea are needed. In this way, the model allows to refine the isotope age curves of ocean sulfate presented in previous papers (Holser and Kaplan, 1966; Nielsen, 1972; Claypool et al., 1980), that are based on a mean of measurements or corrections with respect to a closed-system evaporation. The present work also shows that the  $\delta^{34}\text{S}$  and  $\delta^{18}\text{O}$  values of sulfates from highly evaporated facies (potash-bearing facies), and those involving recycling of sulfates from other ages should not be considered in the calculation of the isotopic composition of seawater sulfate.

**Acknowledgments**—This work was supported by the Spanish Government DGICYT PB94-0163 and AMB93-0220 Projects, by a contract from ENRESA (Empresa Nacional de Residuos Radiactivos, Spain) and by a Collaborative Project between CSIC (Spain) and CNRS (France). Access to the Biurrun borehole and to Subiza mine was granted by J. M. Montes (Potasas de Navarra, SA) to whom we are greatly indebted. J. García-Veigas helped with the sulfate sampling. C. Docherty corrected the English. The critical reviews of H. R. Krouse, W. E. Sanford, and an anonymous reviewer improved the first manuscript. The isotope analyses of sulfates were performed at the Laboratoire d'Océanographie Dynamique et Climatologie, Université Pierre et Marie Curie, Paris.

**Editorial handling:** M. A. McKibben

## REFERENCES

- Ayora C., García-Veigas J., and Pueyo J. J. (1994) The chemical and hydrological evolution of an ancient potash-forming evaporite ba-

- sin as constrained by mineral sequence, fluid inclusion composition and numerical simulation. *Geochim. Cosmochim. Acta* **58**, 3379–3394.
- Birnbaum S. J. and Coleman N. (1979) Source of sulphur in the Ebro Basin (Northern Spain). Tertiary non marine evaporite deposits as evidenced by sulphur isotopes. *Chem. Geol.* **25**, 163–168.
- Busquets P. et al. (1986) *Evaporite Deposition and Diagenesis in the Saline (Potash) Catalan Basin, Upper Eocene*. 6th European Meeting of Sedimentology, Field Trip Guide 1, 13–59.
- Claypool G. E., Holser W. T., Kaplan I. R., Sakai H., and Zak I. (1980) The age curves of sulfur and oxygen isotopes in marine sulfate and their mutual interpretation. *Chem. Geol.* **28**, 199–260.
- Crerar D. A. (1975) A method for computing multicomponent equilibria based on equilibrium constants. *Geochim. Cosmochim. Acta* **39**, 1375–1384.
- Dellwig L. F. (1955) Origin of the Salina salt of Michigan. *J. Sediment Petrol.* **25**, 83–110.
- Filly A., Letolle R., and Puset M. (1975) L'analyse isotopique du soufre. Aspects techniques. *Analusis* **3**, 197–200.
- Fontes J. Ch., Filly A., Gaudant J., and Düringer P. (1991) Origine continentale des évaporites paléogènes de Haute Alsace: arguments paléocéologiques, sédimentologiques et isotopiques. *Bull. Soc. Géol. France* **162**, 725–737.
- Fritz P., Basharmal G. M., Drimmie R. J., Ibsen J., and Qureshi R. M. (1989) Oxygen isotope-exchange between sulphate and water during bacterial reduction of sulphate. *Chem. Geol.* **79**, 99–105.
- Harvie C. H., Moller N., and Weare H. (1984) The prediction of mineral solubilities in natural waters: The Na–K–Mg–Ca–H–Cl–SO<sub>4</sub>–OH–HCO<sub>3</sub>–CO<sub>3</sub>–CO<sub>2</sub>–H<sub>2</sub>O system to high ionic strengths at 25°C. *Geochim. Cosmochim. Acta* **48**, 723–751.
- Holland H. D., Lazar B., and McCaffrey M. (1986) Evolution of the atmosphere and oceans. *Nature* **320**, 27–33.
- Holser W. T. and Kaplan I. R. (1966) Isotope geochemistry of sedimentary sulfates. *Chem. Geol.* **1**, 93–135.
- Holt B. D. and Kumar R. (1991) Oxygen isotope fractionation for understanding the sulphur cycle. In *Stable Isotopes: Natural and Anthropogenic Sulphur in the Environment* (ed. H. R. Krouse and V. A. Grinenko), pp. 27–41. Wiley.
- Krouse H. R. (1980) Sulphur isotopes in our environment. In *Handbook of Environmental Isotope Geochemistry, Vol. 1: The Terrestrial Environment, A* (ed. P. Fritz and J. Ch. Fontes), pp. 435–471. Elsevier.
- Lloyd R. M. (1968) Oxygen isotope behavior in the sulfate-water system. *J. Geophys. Res.* **73**, 6099–6110.
- Longinelli A. (1989) Oxygen 18 and Sulphur-34 in dissolved oceanic sulphate and phosphate. In *Handbook of Environmental Isotope Geochemistry, Vol. 3: The Marine Environment, A* (ed. P. Fritz and J. Ch. Fontes), pp. 435–471. Elsevier.
- Longinelli A. and Craig H. (1967) Oxygen-18 variations in sulfate ions in sea-water and saline lakes. *Science* **156**, 1431–1438.
- Mizutani Y. and Rafter T. A. (1973) Isotopic behaviour of sulphate oxygen in the bacterial reduction of sulphate. *Geochem. J.* **6**, 183–191.
- M. O. P. U. (1990) *Análisis de calidad de aguas 1988–89*. Ministerio de Obras Públicas y Urbanismo de España.
- Nielsen H. (1972) Sulphur isotopes and the formation of evaporite deposits. In *Geology of Saline Deposits* (ed. G. Richter Bernburg), pp. 91–102. Proc. Hannover Symposium.
- Nielsen H. (1978) Sulfur isotopes in nature. In *Handbook of Geochemistry* (ed. K. H. Wedepohl), *Handbook of Geochemistry* 16-B, 1–48.
- Nielsen H. and Ricke W. (1964) Schwefel-isotopen Verhältnisse von Evaporiten aus Deutschland. Ein Beitrag zur Kenntnis von  $\delta^{34}\text{S}$  im Meerwasser-Sulfat. *Geochim. Cosmochim. Acta* **28**, 577–591.
- Nielsen H., Pilot J., Grinenko L. N., Grinenko V. A., Lein A. Yu., Smith J. W., and Pankina R. G. (1991) Lithospheric sources of sulphur. In *Stable Isotopes: Natural and Anthropogenic Sulphur in the Environment* (ed. H. R. Krouse and V. A. Grinenko), pp. 65–132. Wiley.
- Pierre C. (1985) Isotopic evidence for the dynamic redox cycle of dissolved sulphur compounds between free and interstitial solutions in marine salt pans. *Chem. Geol.* **53**, 191–196.
- Pierre C. (1989) Sedimentation and diagenesis in restricted marine basins. In *Handbook of Environmental Isotope Geochemistry, Vol. 3: The Marine Environment, A* (ed. P. Fritz and J. Ch. Fontes), pp. 57–315. Elsevier.
- Pueyo J. J. (1975) Estudio petrológico y geoquímico de los yacimientos potásicos de Cardona, Suria, Sallent y Balsareny (Barcelona, España). Memoria Tesis Doctoral, Univ. Barcelona.
- Puigdefábregas C. (1975) *La sedimentación molásica en la cuenca de Jaca*. Mon. Instituto Estudios Pirenaicos, CSIC, 104.
- Raab M. and Spiro B. (1991) Sulfur isotopic variations during sea water evaporation with fractional crystallization. *Chem. Geol.* **86**, 323–333.
- Rafter T. A. and Mizutani Y. (1967) Preliminary study of variation of oxygen and sulphur isotope in natural sulphates. *Nature* **216**, 1000–1002.
- Rosell L. (1983) Estudi petrològic, sedimentològic i geoquímic de la formació de sals potàssiques de Navarra (Eocè superior). Memoria Tesis Doctoral. Univ. Barcelona.
- Sanford W. E. and Wood W. W. (1991) Brine evolution and mineral deposition in hydrologically open evaporite basins. *Amer. J. Sci.* **291**, 687–710.
- Sonnenfeld P. (1984) *Brines and Evaporites*. Academic Press.
- Taylor B. E., Wheeler M. C., and Norstrom D. K. (1984) Stable isotope geochemistry of acid mine drainage: Experimental oxidation of pyrite. *Geochim. Cosmochim. Acta* **48**, 2669–2678.
- Thode H. G. and Monster J. (1965) Sulphur isotope geochemistry of petroleum, evaporites and ancient seas. In *Fluids in Subsurface Environments* (ed. A. Young and J. E. Galley); *AAPG Mem.* **4**, 367–377.
- Utrilla R., Pierre C., Orti F., and Pueyo J. J. (1992) Oxygen and sulphur isotope composition as indicators of the origin of Mesozoic and Cenozoic evaporites from Spain. *Chem. Geol.* **102**, 229–244.
- Van Everdingen R. O. and Krouse H. R. (1985) Isotope composition of sulphates generated by bacterial and biological oxidation. *Nature* **315**, 395–396.